



HAL
open science

Seasonal Variations, Origin, and Parameterization of Ice-Nucleating Particles at a Mountain Station in Central France

Yannick Bras, Evelyn Freney, Antoine Canzi, Pierre Amato, Laetitia Bouvier, Jean-Marc Pichon, David Picard, María. Cruz Minguillón, Noemí Pérez, Karine Sellegri

► **To cite this version:**

Yannick Bras, Evelyn Freney, Antoine Canzi, Pierre Amato, Laetitia Bouvier, et al.. Seasonal Variations, Origin, and Parameterization of Ice-Nucleating Particles at a Mountain Station in Central France. *Earth and Space Science*, 2024, 11, 10.1029/2022EA002467 . insu-04763962

HAL Id: insu-04763962

<https://insu.hal.science/insu-04763962v1>

Submitted on 3 Nov 2024

HAL is a multi-disciplinary open access archive for the deposit and dissemination of scientific research documents, whether they are published or not. The documents may come from teaching and research institutions in France or abroad, or from public or private research centers.

L'archive ouverte pluridisciplinaire **HAL**, est destinée au dépôt et à la diffusion de documents scientifiques de niveau recherche, publiés ou non, émanant des établissements d'enseignement et de recherche français ou étrangers, des laboratoires publics ou privés.



Distributed under a Creative Commons Attribution - NonCommercial - NoDerivatives 4.0 International License








RESEARCH ARTICLE

10.1029/2022EA002467

Special Collection:

Land-atmosphere coupling: measurement, modelling and analysis

Seasonal Variations, Origin, and Parameterization of Ice-Nucleating Particles at a Mountain Station in Central France

Yannick Bras¹ , Evelyn Freney¹ , Antoine Canzi¹, Pierre Amato² , Laetitia Bouvier¹, Jean-Marc Pichon¹, David Picard¹ , María Cruz Minguillón³, Noemí Pérez³ , and Karine Sellegri¹ 

¹Laboratoire de Météorologie Physique, UMR6016, Université Clermont Auvergne-CNRS, Aubière, France, ²UMR6296, Institut de Chimie de Clermont-Ferrand, Université Clermont Auvergne-CNRS, Aubière, France, ³Institute of Environmental Assessment and Water Research, Barcelona, Spain

Key Points:

- Size-segregated airborne ice-nucleating particles (INP) concentrations were measured at an altitude station in Central France over 6 months
- Seasonal variations are observed with a minimum in winter. The majority of INPs is biological and activated above -18°C
- We developed a parameterization for predicting INP concentrations at warm temperatures based on total aerosol concentrations

Supporting Information:

Supporting Information may be found in the online version of this article.

Correspondence to:

E. Freney and K. Sellegri,
evelyn.freney@uca.fr;
Karine.Sellegri@opgc.cnrs.fr

Citation:

Bras, Y., Freney, E., Canzi, A., Amato, P., Bouvier, L., Pichon, J.-M., et al. (2024). Seasonal variations, origin, and parameterization of ice-nucleating particles at a mountain station in Central France. *Earth and Space Science*, 11, e2022EA002467. <https://doi.org/10.1029/2022EA002467>

Received 14 JUN 2022

Accepted 21 MAR 2024

Author Contributions:

Conceptualization: Yannick Bras,

Evelyn Freney, Karine Sellegri

Data curation: Yannick Bras,

Evelyn Freney, Laetitia Bouvier, Jean-

Marc Pichon, David Picard, María

Cruz Minguillón, Noemí Pérez

Abstract Identifying how aerosol particles interact with atmospheric water is critical to understand climate and precipitation. Ice-nucleating particles (INP) trigger the formation of atmospheric ice crystals at higher temperatures than pure water. They are difficult to characterize because of their scarce occurrence, and variability, in the atmosphere, especially at temperatures above -20°C . It has been demonstrated that at these temperatures, biological aerosol particles can contribute significantly to INP number concentration. This study incorporates a series of offline, size-segregated measurements of INPs collected at the Puy de Dôme station (PUY, 1,465 m a.s.l.) over a 6 month period from October to May, covering the transitions from autumn, winter, to spring. These measurements show a general trend of decreasing particle number concentrations during the winter months and higher concentration during autumn and spring. INP concentrations measured in the range of -5 and -18°C , had concentrations of 0.001 INP/ L_{air} at the warmest temperatures, and between 0.01 and 0.1 INP/ L_{air} at the coldest temperatures. The majority of INP measured at temperatures warmer than -15°C were heat labile, suggesting a biological or organic origin. The INP variability was compared with collocated aerosol physical and chemical properties, allowing us to associate highest INP concentrations with local and marine origins. Following these comparisons, we use aerosol total number concentration to develop a new parameterization. In addition, this parameterization is specifically optimized for warmer temperature INP measurements, and demonstrated a good performance when tested on independent data sets.

Plain Language Summary Understanding how tiny particles in the air (aerosol particles) interact with water in the atmosphere is crucial for studying climate and precipitation. Ice Nuclei Particles (INP) play a role in forming ice crystals in the atmosphere, especially at higher temperatures. This is important because it's been found that biological aerosol particles can significantly contribute to INP at temperatures above -20°C . The study conducted offline measurements of INPs over 6 months at the Puy de Dôme station, covering the transition from autumn to spring. Results showed a general trend of fewer particles during winter and more during autumn and spring. The INP concentrations were highest at temperatures between -5 and -18°C , with warmer temperatures having 0.001 INP per liter of air and colder temperatures having 0.01 to 0.1 INP per liter of air. Most INPs at temperatures above -15°C were heat-sensitive, indicating a biological or organic origin. This study linked high INP concentrations to local and marine sources by comparing them with aerosol properties. A new parameterization based on total aerosol number concentration, specifically optimized for warmer temperatures, performed well when tested on independent data sets.

1. Introduction

Atmospheric aerosol particles have a wide range of physical and chemical properties. Knowing how these aerosol particles interact with atmospheric water vapor is critical to assessing their impact on the Earth's energy balance and on the atmospheric water cycle (Boucher & Randall, 2013; D. Hartmann et al., 1992; Lohmann & Feichter, 2005).

In clouds at temperatures above -38°C , aerosol particles can induce heterogeneous freezing and lead to the formation of atmospheric ice crystals (Pruppacher, 2010) by reducing the energy barrier required by the ice nucleation process. These aerosols are referred to as ice-nucleating particle (INPs). INPs are very scarce in the atmosphere, with concentrations usually ranging from 0.1 to 10 L^{-1} (while the total concentration of aerosols is ranging from 10^5 to 10^7 L^{-1}), thus making them difficult to detect and quantify, and therefore to understand.

© 2024. The Author(s).

This is an open access article under the

terms of the [Creative Commons](https://creativecommons.org/licenses/by/4.0/)

[Attribution-NonCommercial-NoDerivs](https://creativecommons.org/licenses/by/4.0/)

License, which permits use and

distribution in any medium, provided the

original work is properly cited, the use is

non-commercial and no modifications or

adaptations are made.

Formal analysis: Yannick Bras, Evelyn Freney, Antoine Canzi, Noemí Pérez, Karine Sellegri
Funding acquisition: Evelyn Freney
Investigation: Yannick Bras, Evelyn Freney, Karine Sellegri
Methodology: Yannick Bras, Evelyn Freney, Antoine Canzi, Pierre Amato, Noemí Pérez, Karine Sellegri
Project administration: Evelyn Freney, Karine Sellegri
Resources: Evelyn Freney, Karine Sellegri
Supervision: Evelyn Freney, Karine Sellegri
Validation: Evelyn Freney, Karine Sellegri
Visualization: Yannick Bras
Writing – original draft: Yannick Bras, Pierre Amato
Writing – review & editing: Evelyn Freney, Pierre Amato, Karine Sellegri

Furthermore, depending on their nature, INPs in the mixed-phase cloud regime are active at different ranges of temperatures between 0 and -38°C . Some specific aerosol particles identified as having good ice-nucleating abilities include mineral dust, soil dust, and primary biological aerosol particles (Kanji et al., 2017), either of terrestrial origin (Schneider et al., 2021) or of marine origin (McCluskey et al., 2017; Wilson et al., 2015). Dust-derived particles have been identified as the dominant INP type at temperatures below -20°C , whereas biological aerosols such as bacteria or fungal spores are the dominant INP types identified active at temperatures above -15°C (Huang et al., 2021; Kanji et al., 2017; Maki et al., 1974). It has also recently been illustrated that biogenically derived secondary organic aerosols could also have ice nucleating properties in cirrus freezing regimes (Wolf et al., 2020).

Another element of uncertainty in our current view of ice nucleation in the atmosphere are the different pathways by which an ice crystal may form. These pathways, or activation modes, are described in detail by Kanji et al. (2017). There are generally four different modes considered in the literature (deposition ice nucleation, contact freezing, immersion freezing and condensation freezing; see Kanji et al. (2017) for a thorough description of each mode). Different INP sampling instruments can often only operate in one or two ice nucleation modes, which is another obstacle to making and comparing INP measurements.

To date, there is not one instrumental method that can characterize INPs across the full temperature range between 0 and -38°C . Different sampling and analytical procedures, both online and offline, have been widely used in the past and therefore reproducibility of instrumental methods in both controlled (DeMott et al., 2018) and ambient conditions (Lacher et al., 2024) is essential (DeMott et al., 2011). Online methods allow the measurement of INP concentrations with high time resolution (seconds to minutes), making it possible to follow the high temporal variability of ambient INP concentrations. Current online instruments operate at temperatures colder than -15°C and provide much needed information on the temporal variability of INPs. However, due to low INP concentrations, they often need to be operated downstream of a particle concentrator (Gute et al., 2019). Offline methods are low cost, and generally easier to deploy at different sampling sites. As samples are accumulated over longer periods of time, they allow examination of low concentrations of INPs. Therefore making them more effective than online measurements for studying biological INPs.

In the last decade, significant technological advances have been made in the development of new measurement methods for atmospheric INP, leading to a substantial increase in the number of field campaigns aimed at answering scientific questions on the sources and variability of INPs in different atmospheric environments. However, only a few studies focused on analyzing INP seasonal trends and variability (M. Hartmann et al., 2019; Pouzet et al., 2017; Schneider et al., 2021; Schrod et al., 2020; Wex et al., 2015). These studies have shown an increased number of INP in the spring and summer, but seasonal data is still lacking in different types of environments.

It is essential to have these long-term INP data sets if we are to derive accurate parameterizations that will predict INP from aerosol properties under different atmospheric conditions and environments. This will allow them to be incorporated into global numerical models to study and predict climate and precipitation more accurately Burrows et al. (2022). Historically, the most commonly used INP parameterizations are those based on temperature since it is easier to implement into numerical models without needing additional measurements (Fletcher, 1962; Meyers et al., 1992). With the increase in collocated measurements of ambient aerosols and INP properties, a number of parameterizations have been developed using a wide range of parameters. Some parameterizations use aerosol number concentration (DeMott et al., 2010, 2015; Tobo et al., 2013), others use aerosol surface concentration (Ullrich et al., 2017), or aerosol chemical properties (Niemand et al. (2012) for dusts, Atkinson et al. (2013) for feldspar, Wex et al. (2015) and Patade et al. (2021) for biological materials). However, a major drawback from the majority of these parameterizations is that they have been optimized for temperatures below -20°C and therefore do not accurately predict INP concentrations at warmer temperatures (Huang et al., 2021; Schneider et al., 2021).

Due to the huge variability in INP types and properties between the different regions of the globe, there is a strong motivation to increase the number of field studies (Huang et al., 2021; Kanji et al., 2017; Murray et al., 2012), especially at warm temperatures ($>-20^{\circ}\text{C}$), in order to increase data availability and to better understand ice nucleation by biological aerosols. In this context, measurements were performed during the Puy de Dôme Ice Nucleation Intercomparison Campaign (PICNIC) at the summit of the Puy de Dôme Mountain (PUY, 1465 m.a.s.l.) in Central France in October 2018. In addition to characterizing INP concentrations and variability at a high altitude remote station, this field campaign had a second objective to compare a range of both offline and online

ice nucleation measurement techniques in ambient environments (Lacher et al., 2024). After PICNIC, weekly size resolved filters were collected for analysis of INP concentrations until May 2019.

In this work, an overview is provided for INP measurements at PUY, including their concentrations, seasonal variability, and relation with aerosol physical and chemical properties. Using a combination of these measurements, we propose a parameterization optimized for warm temperature ($> -20^{\circ}\text{C}$) INP activity. We then test this parameterization on two independent data sets.

2. Methods

2.1. Site Description and Instrumental Setup

The Puy de Dôme station (PUY) is located at the top of the Puy de Dôme mountain ($45^{\circ}46'$ N, $2^{\circ}57'$ E, 1,465 m a.s.l.) in central France. The site is influenced by long range air masses from both the continental and oceanic sectors (Baray et al., 2020; Farah et al., 2018). Given both its altitude and surrounding geography this site can be situated occasionally in the lower free troposphere, making it an interesting site to study the properties of different atmospheric layers (Farah et al., 2018; Freney et al., 2016). The PUY site is identified as a global atmospheric watch (GAW) station as well as being an Aerosol, Clouds and Trace Gases Research Infrastructure (ACTRIS) facility. A detailed description of the station is available in Baray et al. (2020). In addition to the measurement of continuous meteorological parameters (temperature, humidity, and pressure), the station is equipped with a wide range of both online and offline measurement methods, to study in-situ gas and aerosol properties.

For this work, we use measurements of aerosol size and number concentration using a custom made Scanning Mobility Particle Sizer (SMPS) (Figure S1 in Supporting Information S1) coupled with a condensation particle counter (CPC 3010, TSI) measuring particle diameters from 10 nm up to 600 nm. An optical particle counter (OPC, Grimm model 1.108) was measuring supermicronic aerosol number concentration from sizes 0.3–20 μm . However, due to poor data coverage (Figure S2 in Supporting Information S1) only measurements from the SMPS will be used. Only total aerosol number concentrations ($N_{aer,tot}$ representing sizes from 10 nm up to 600 nm), number concentrations of aerosols with diameters greater than 500 nm ($N_{aer,500}$) and the aerosols surface area ($S_{aer,tot}$) and surface measured by the SMPS are used in this study (Picard, 2021). The Magee Scientific Aethalometer[®] AE33 was used for black carbon measurement. Filter based aerosol chemistry measurements were obtained from a high volume sampler located on the rooftop of the station.

Concentrations of INPs were measured during two consecutive periods with different sampling procedures. During the PICNIC campaign (starting from 9 October 2018 to 24 October 2018), high-volume filter samples (1,160 L/min, total volume sampled: $\approx 557\text{ m}^3$) were taken on 147 mm diameter quartz filters every day (from 10:00 to 18:00) and night (from 22:00 to 06:00). Prior to analysis, the filters were conserved at -10°C in the laboratory for 2–3 months. We are aware that studies have suggested that INP activity may decrease somewhat if the analysis is not performed immediately (e.g., “Best practices for precipitation sample storage for offline studies of ice nucleation in marine and coastal environments” (Beall et al., 2020)). We can therefore consider these samples to the lower limit of ice nucleation activity.

After the PICNIC campaign, a period of Weekly Ice Nuclei Samples (WINS) were collected from 7 November 2018 to 25 May 2019. A 4-stage Dekati[®] impactor and 25 mm diameter quartz filters were used for size segregated INP measurements, with size bins of 0.1–1, 1–2.5, 2.5–10, and $>10\text{ }\mu\text{m}$. Contrary to PICNIC, the sampling was done from inside the observatory behind a whole air aerosol inlet (WAI) with a 50% cut-size diameter of 25 μm (for wind speeds of 7 m s^{-1}) and a flow rate of 10 L/min. Samples were collected continuously over a 7 day period, resulting in one size segregated sample per week. The chemical properties of the aerosols during the sampling periods were analyzed using the same filters as those used for the INP analysis. Chemical analysis of the filters was performed using ion chromatography using the method described by Bourcier et al. (2012), thus providing mass concentrations of anions (Cl^- , NO_3^- , SO_4^{2-} , Oxalate) and cations (Na^+ , NH_4^+ , K^+ , Mg^{2+} , Ca^{2+}). As a result of the long sampling times used during WINS, it was not possible to study the impact of specific air masses on the INP concentrations, therefore we use the chemical composition of the aerosols particles as a proxy for the air masses at PUY (Farah et al., 2018).

In parallel to the PICNIC campaign, a number of other European sites collected filter samples for INP analysis. In this study, we used quartz filter measurements from the ACTRIS station Montsec d'Ares (MSA; 42°3'N, 0°44'E, 1,570 m a.s.l.). Those filters were collected by the Institute of Environmental Assessment and Water Research (IDAEA), Barcelona, Spain. The 24 hr filter samples (Quartz microfiber filters) were collected with a high-volume sampler (30 m³ h⁻¹, MCV CAV-A/Msb) behind a PM10 head. The RH in the sample inlet was monitored continuously and was always inferior to 50%. Similarly to PUY, MSA is a continental background altitude site (Ripoll, Minguillón, et al., 2014; Ripoll, Pey, et al., 2014). The atmospheric conditions at MSA are characteristic of Mediterranean climate with local and regional atmospheric air masses and Saharan dust inclusions (Ealo et al., 2016; Ripoll, Minguillón, et al., 2014; Ripoll, Pey, et al., 2014). These data sets were used to evaluate the newly developed parameterization (Section 5).

2.2. Ice-Nucleating Particles Analysis

INP analysis of offline filters were made with the LED-based Ice Nucleation Detection Apparatus (LINDA) technique (Stopelli et al., 2014), an offline method used to analyze samples of INP and their properties in the immersion freezing mode (Hiranuma et al., 2019; Pouzet et al., 2017).

LINDA consists of a network of LEDs underneath an array of 52 Eppendorf® tubes filled with a 0.9% NaCl solution containing INPs. It is recommended to prepare samples in a 0.9% NaCl solution (equal to physiological solution) for sample stability and to avoid an eventual osmotic stress on biological material. A series of tests using several salt concentrations were performed by Stopelli et al. (2014), and for this range of salt concentrations had no noticeable impact on the freezing temperatures.

The array of tubes is placed in a cooling bath, with a temperature probe at each corner. An USB CMOS Monochrome Camera placed above the array allows detecting the freezing of the tubes by the variation of the intensity of the light transmitted through the tubes. The temperature in the cooling bath was decreased at a rate of -0.33°C/min.

For the analysis with LINDA, punches of the filters (4.5 cm² for PICNIC, 4.3 cm² for WINS) were washed in a 25 mL solution of 0.9% NaCl during 20 min by agitation, then half of the tubes (26 tubes) were filled using the resulting solution (200 µL in each tube). The remaining solution was then heated for 30 min in boiling water at 100°C, and was used to fill the remaining 26 tubes of LINDA array. The purpose of this heat treatment is to remove the biological contribution to the INP, a widely used method in the community (Christner et al., 2008; O'Sullivan et al., 2018; Wilson et al., 2015). This is supported by the fact that most biological INPs active at such high temperatures are composed of proteinaceous material, such as bacteria (Huang et al., 2021), and are thus heat-labile. In the following discussion, we refer to the INPs from heated samples as "Heat Stable" (HS) INPs and the difference between untreated and heated samples as "Heat Labile" (HL) INP concentrations.

The cumulative INP concentration n_{INP} were calculated using the Vali (1971) formula:

$$n_{\text{INP}} = \frac{\ln N_0 - \ln N(T)}{V}, \quad (1)$$

where N_0 is the total number of droplets (here the number of Eppendorf tubes, 26), $N(T)$ is the number of droplets frozen at temperature T and V is the volume of a droplet (here, $V = 200$ µL).

For filter samples, the number of INP per mL of liquid analyzed are converted to the number of INP per volume of air, using Equation 2:

$$n_{\text{INP}}^{\text{air}} = \frac{n_{\text{INP}}^{\text{mL}} \cdot S_F V_{\text{dil}}}{V_{\text{air}} S_P}, \quad (2)$$

where $n_{\text{INP}}^{\text{air}}$ and $n_{\text{INP}}^{\text{mL}}$ are INP concentrations per liter of air and per mL of solution, respectively. V_{air} is the volume of air sampled for each filter in L, S_F the total surface of the sampling filter in cm², $V_{\text{dil}} = 25$ mL the volume used for washing the filter, S_P the surface of punches of filter used for the analysis in cm².

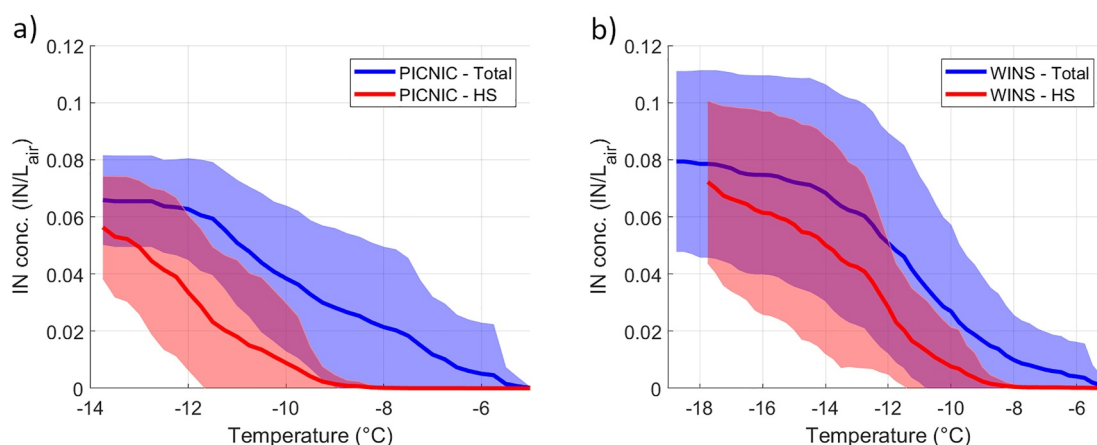


Figure 1. Cumulative ice-nucleating particles concentrations at PUY during the (a) Puy de Dôme Ice Nucleation Intercomparison Campaign (PICNIC) campaign, (b) weekly ice nuclei samples (WINS) campaign for INP_{tot} (blue), INP_{HS} (red). The solid line corresponds to the mean, the shaded area corresponds to one standard deviation. The number of samples is $N = 21$ for PICNIC and $N = 19$ for WINS.

Blank filters were handled and analyzed through the same procedure in order to estimate background errors. On average, blank samples started freezing at approximately -10°C , but remained consistently below the filter samples until about -18°C (Figure S3 in Supporting Information S1). PICNIC blanks were generally higher than WINS blanks, and all tubes were frozen at -15°C , instead of about -19°C for WINS blanks. Heating did not change the freezing profile of blank samples. All figures show the INP concentrations corrected for background concentrations using their corresponding blank samples.

3. General Observations and Time Series

3.1. General Features of the INP Concentrations

The cumulative INP temperature spectra for both campaigns are shown for all samples in Figure 1, and represented using all data points in Figure S4 in Supporting Information S1, and as boxplots in Figure S5 in Supporting Information S1. Heat stable (HS) INPs are defined as the heated samples, while heat labile (HL) INP concentrations were calculated as the difference between the unheated and heated samples. In both field campaigns, the total INP concentrations (unheated samples) vary between 10^{-4} INP/stdL to 10^{-1} INP/stdL at the highest temperatures, and are around 10^{-1} INP/stdL at the coldest temperatures. Both data sets show similar freezing onset, around $-6 \pm 1^{\circ}\text{C}$, but all samples are activated for PICNIC at -14 and at -18°C for WINS. The high activation temperature from the PICNIC field campaign is a result of higher particle loads, and hence high INP concentrations, on the filters. Additional dilutions would have increased the range of temperatures available for this sample set. These values are comparable with global INP data (Conen et al., 2022; DeMott et al., 2018; Ladino et al., 2019; Tobo et al., 2019).

A clear decrease in INP numbers is visible after the heat treatment, indicating a large fraction of INP as heat-labile INPs (Figure 1), which suggests the presence of particles of biological origin containing proteinaceous ice-active material (Christner et al., 2008; T. C. Hill et al., 2016; Huang et al., 2021). These concentrations ranged from 10^{-4} INP/stdL to 10^{-2} INP/stdL at the higher temperatures ($> -10^{\circ}\text{C}$), from 10^{-2} to 10^{-1} INP/stdL at the lowest temperatures ($< -10^{\circ}\text{C}$). For both data sets, the heat treatment decreases the freezing onset of the samples by about $3\text{--}4^{\circ}\text{C}$. At temperatures above -10°C , about 80%–90% of the observed IN activity can be attributed to biological origins, which is in line with other studies on cloud water (Joly et al., 2014), snow (T. C. J. Hill et al., 2014) or rain water (Lu et al., 2016). At warmer temperatures ($> -10^{\circ}\text{C}$), as a result of lower INP activity, much higher variability is observed compared to the colder temperatures, represented by the outliers in Figure S5 in Supporting Information S1. At -12°C , an average of 36% of INPs are heat labile for PICNIC, and 62% for WINS. At -18°C , less than 10% of all INPs are heat labile, consistent with other studies that used heat treatment for differentiating heat labile biological INPs in different types of environments (Conen et al., 2022; Joly et al., 2014; T. C. J. Hill et al., 2014; McCluskey et al., 2018; O'Sullivan et al., 2018; Schrod et al., 2020), showing that biological INP are responsible for early onset freezing.

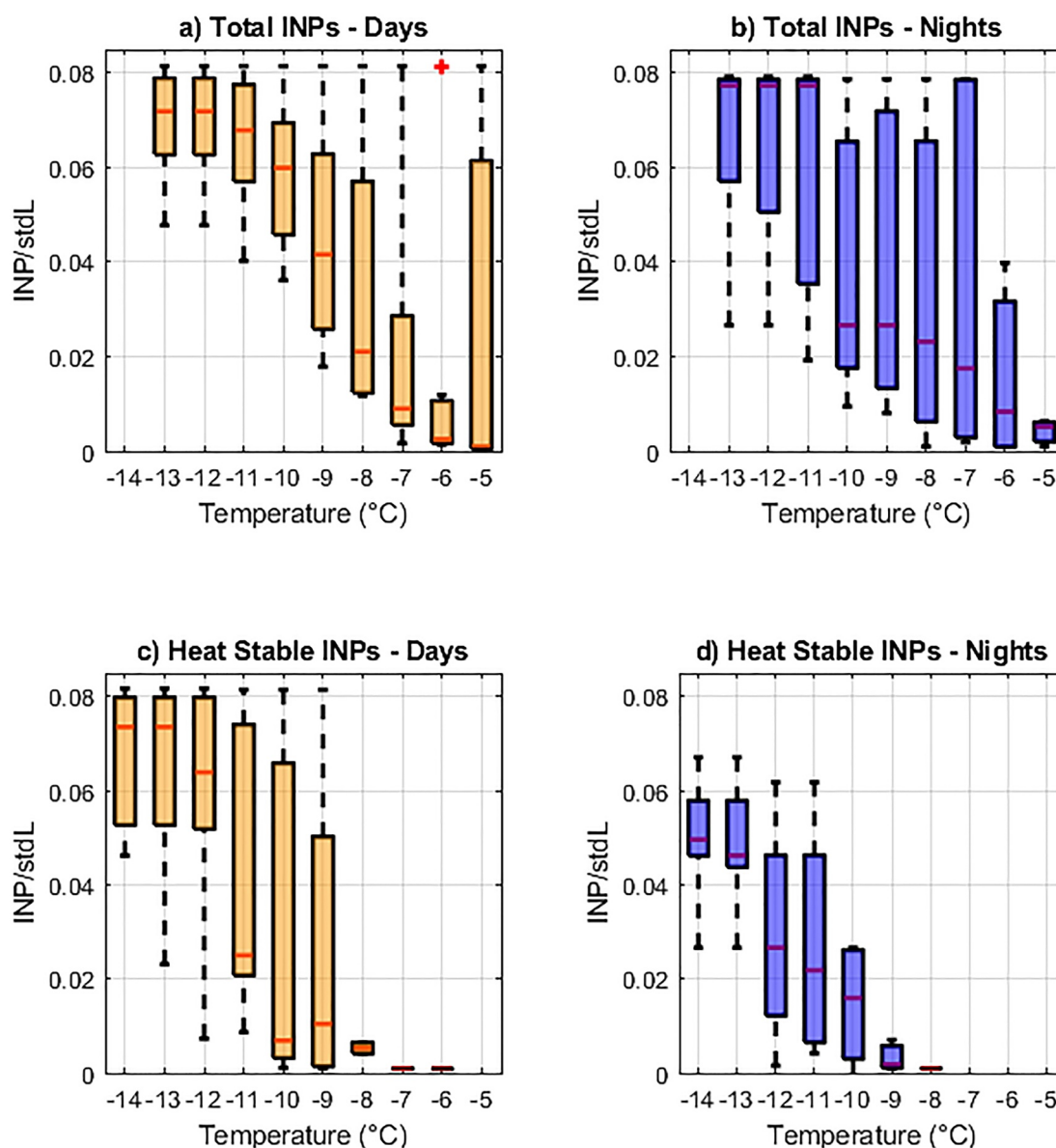


Figure 2. Differences between day-time and night-time concentrations of total and heat stable ice-nucleating particles concentrations during Puy de Dôme Ice Nucleation Intercomparison Campaign. Night and day values corresponds respectively to the periods 22:00 to 06:00 and 10:00 to 18:00. Night values were calculated using 10 samples, day values were calculated using 11 samples.

3.2. Day-Night Contrast During PICNIC

The average day-night concentrations of total and HS INP concentrations measured during the PICNIC experiment are shown in Figure 2. The median concentrations of total INPs (Figures 2a and 2b) are generally the same at night as during the day, but the interquartile range (25%–75%, materialized by the boxes in Figure 2) is higher at night, showing increased variability of INP concentrations. The concentrations of HS INPs (Figures 2c and 2d) are consistently higher during day time than night time. This is particularly the case at colder temperatures ($<-12^{\circ}\text{C}$), where the difference is about 0.03 INP/stdL. This suggests that the contribution of HL INPs to the total INPs is higher at night than during the day.

This is potentially a result of the increased abundance of particles of biological origin during the night, a phenomenon already observed at PUY by Gabey et al. (2013). This phenomenon of larger particles measured in higher concentrations during free tropospheric conditions (and nighttime periods) was discussed by Farah

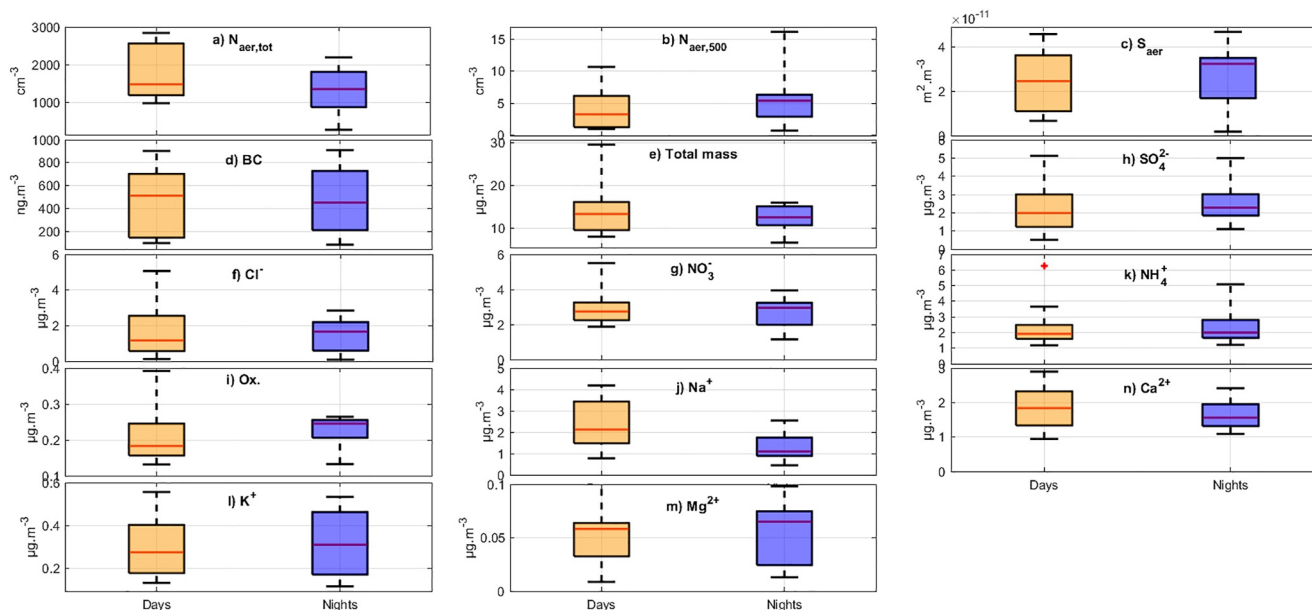


Figure 3. Day night variations of physical and chemical parameters at PUY during Puy de Dôme Ice Nucleation Intercomparison Campaign. Night and day values corresponds respectively to the periods 22:00 to 06:00 and 10:00 to 18:00. Night values were calculated using 10 samples, day values were calculated using 11 samples.

et al., 2018; Bourcier et al., 2012 for the PUY. In both papers, it was hypothesized that more efficient long-range transport of larger marine particles/dust (and possibly biological aerosols) may occur at higher altitudes, this is particularly relevant during the winter months when stronger winds are often present.

The day-night difference of other aerosol parameters were also computed to investigate their relationship with the INP trends (Figure 3). $N_{aer,tot}$ increases by 22% on average from night to day, which is in line with the trends of HS INPs. The variation in total aerosol is similar to observations from Venzac et al. (2009), where autumn diurnal aerosol concentration varied from 1,100 to 2,800 cm^{-3} . During the day, the increasing boundary layer height means that smaller particles from nearby sources are transported to the site, or those that are formed through particle nucleation processes. On the contrary, $N_{aer,500}$ and S_{aer} increases on average at night, which is in line with the increase of HL INPs at night. At night, the PUY is sampling at the top of the mixing layer or in the residual layer where aerosol concentrations are more often long range transported. S_{aer} does not show a significant variation during the period. For the chemical parameters, Na^+ increases by 44% on average during the day compared with moderate increases from Cl^- , NO_3^- and Ca^{2+} (10%–15%). For SO_4^{2-} , concentrations decreases by 10% during daytime. The other chemical parameters do not show any significant variation (below 5%).

3.3. Seasonal Variations

The weekly time series of INP data (HS and HL) at -8 , -12 , and -15°C and of the collocated measurements are shown in Figure 4. These temperatures correspond respectively to the temperatures at which a majority of HL INPs are activated, at which both HL and HS INP are present in similar concentrations, and at which the majority of all INPs have been activated. PICNIC concentrations are not shown at -15°C , as all INPs were activated above -14°C .

Although the measured number concentrations are low, we observe a trend with lower INP concentrations at PUY for both HL and HS during the winter and higher concentrations measured during spring and autumn (Figures 4a–4c). Similar trends were reported in precipitation water (Pouzet et al., 2017) and in a boreal forest in Finland (Schneider et al., 2021). Higher ratios of HL/total INPs are observed during the winter months, than during the spring or autumn months. However, calculations made during the winter months are based on low concentrations and are subject to high uncertainties. We observe similar seasonal variations of aerosol numbers ($N_{aer,tot}$, $N_{aer,500}$, Figure 4d), surface area (S_{aer} , Figure 4e) and composition (Figures 4f and 4g). The link with $N_{aer,500}$ is consistent with the observations by DeMott et al. (2010), who illustrated that INP concentrations were strongly related with larger particle diameters often related to dust particles.

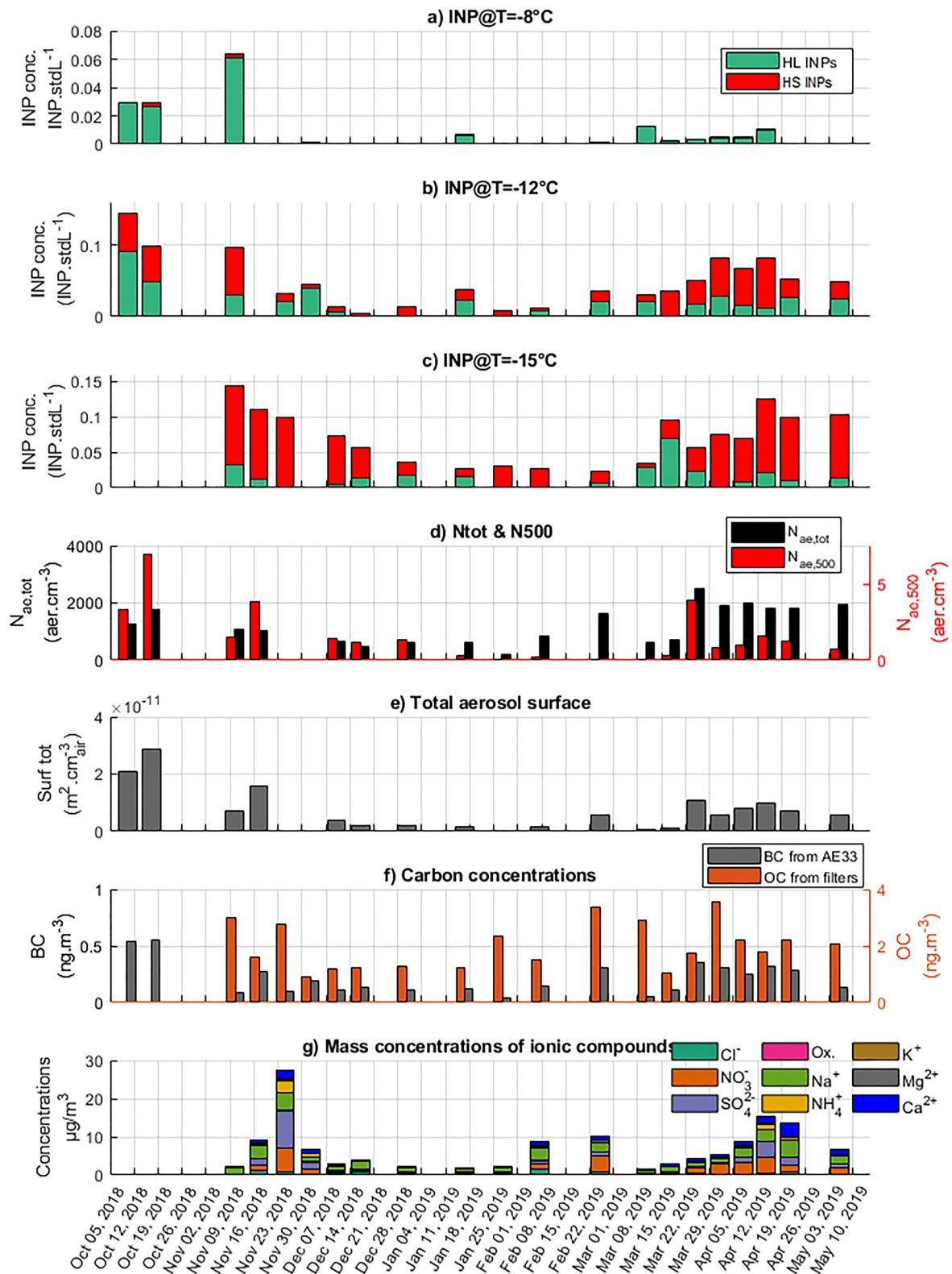


Figure 4. Time series at PUY of weekly averaged data for the Puy de Dôme Ice Nucleation Intercomparison Campaign and Weekly Ice Nuclei Samples sampling period: (a) ice-nucleating particles (INP) data at -8°C , (b) INP data at -12°C , (c) INP data at -15°C , (d) $N_{ae,tot}$ and $N_{ae,500}$ number concentrations (cm^{-3}), (e) Total surface of aerosols ($\text{m}^2/\text{m}^3_{air}$), (f) Carbon concentrations (BC, OC) ($\mu\text{g}/\text{m}^3$), (g) Masses of cations and anions from filters ($\mu\text{g}/\text{m}^3$).

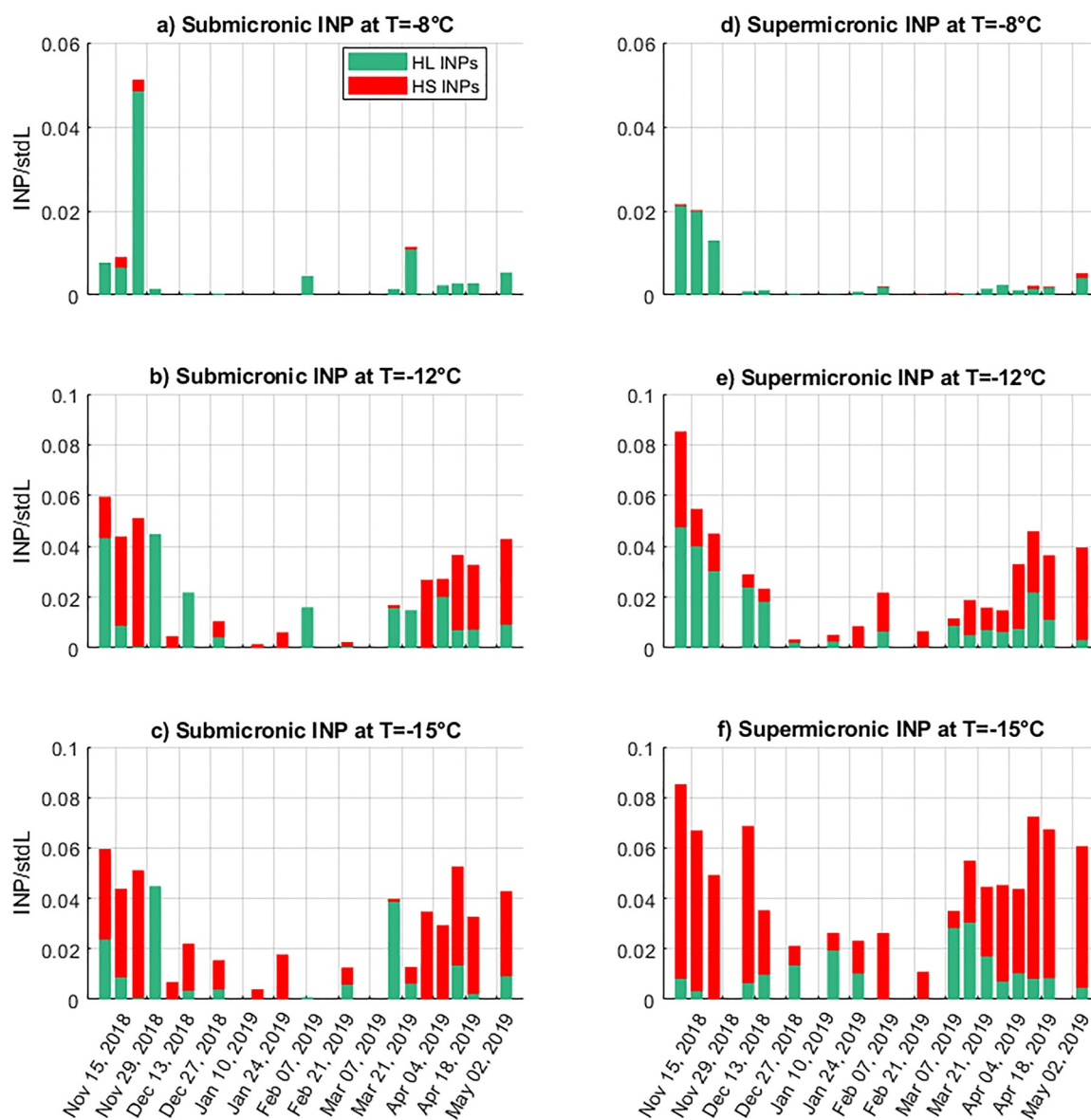


Figure 5. Time series of submicronic (a–c) and supermicronic (d–f) ice-nucleating particles concentrations during weekly ice nuclei samples at $T = -8^{\circ}\text{C}$, $T = -12^{\circ}\text{C}$, and $T = -15^{\circ}\text{C}$.

Furthermore, the seasonal trend in aerosol properties at PUY has previously been reported for aerosol concentrations by Farah et al. (2021), Bourcier et al. (2012), and Venzac et al. (2009). At PUY, this seasonal variation is strongly influenced by the variability in the boundary layer height that does not reach the site as often during winter compared to summer, in agreement with previous studies (Farah et al., 2018; Venzac et al., 2009).

3.4. Size Segregation

During the WINS experiment, size segregated filters were collected, allowing the examination of INP variability for both submicron and supermicron aerosol particles (Figure 5 and Figure S6 in Supporting Information S1). These filters were grouped into submicron and supermicron size categories to ensure sufficient mass concentration for analysis. At all temperatures, both submicron and supermicron INPs show similar seasonal variation with a wintertime minimum. Although the supermicron and submicron aerosol particles have similar (within the uncertainty) INP concentrations, contributing $49.8 \pm 29\%$, $55 \pm 22\%$, and $63 \pm 18\%$ to the total INP number at -8 , -12 , and -15°C respectively, the INP activity of supermicron particles tends to be higher than those of the

Table 1
Linear Regression Correlations Coefficients (R^2) and p -Values (Pearson's Test) Between the Weekly Ice Nuclei Samples Ice-Nucleating Particles (INP) Concentrations at -8 , -12 , and -15°C (INP_{-8} , INP_{-12} , INP_{-15}) and Aerosol Parameters

	$N_{aer,tot}$	$N_{aer,500}$	S_{aer}	BC	Cl^-	NO_3^-	SO_4^{2-}
$INP_{tot,-8}$	0.70 (<0.005)	0.39 (0.01)	0.74 (<0.005)	–	–	0.25 (0.03)	0.61 (<0.005)
$INP_{tot,-12}$	–	–	–	–	–	–	–
$INP_{HS,-12}$	0.40 (0.01)	–	–	–	–	0.24 (0.03)	0.35 (0.01)
$INP_{HL,-12}$	–	–	–	–	–	–	–
$INP_{tot,-15}$	–	–	–	–	–	–	–
$INP_{HS,-15}$	0.28 (0.04)	–	–	–	–	–	0.24 (0.04)
$INP_{HL,-15}$	–	–	–	–	–	–	–
	Ox.	Na^+	NH_4^+	K^+	Mg^{2+}	Ca^{2+}	
$INP_{tot,-8}$	0.73 (<0.005)	0.24 (0.03)	0.60 (<0.005)	0.25 (0.03)	–	–	–
$INP_{tot,-12}$	–	0.24 (0.03)	0.21 (0.05)	–	–	–	–
$INP_{HS,-12}$	–	0.38 (0.01)	0.37 (0.01)	–	–	–	0.33 (0.01)
$INP_{HL,-12}$	–	–	–	–	–	–	–
$INP_{tot,-15}$	–	–	–	–	–	–	–
$INP_{HS,-15}$	–	0.31 (0.02)	0.27 (0.03)	–	–	–	0.22 (0.05)
$INP_{HL,-15}$	–	–	–	–	–	–	–

Note. Only significant ($P < 0.05$) correlations are shown. Values with no significant correlations are indicated as n-dashes. Values with $P < 0.005$ are indicated in bold.

sub micron mode. This is consistent with previous studies showing that INPs are abundant in the supermicron range at temperatures warmer than -20°C . Past studies report that at -15 and -20°C , respectively 80% and 55% of INPs are supermicronic (Creamean et al., 2018; Huffman et al., 2013; Mason et al., 2016).

The ratio of HL to total (and hence thought to be of biogenic origin) INPs at -8 and -12°C is higher by 10% for submicron INPs than for supermicron INPs: the fraction of HL to total INP are $97 \pm 7\%$; $57 \pm 39\%$, and $44 \pm 8\%$ at -8 , -12 , and -18°C respectively in the submicron mode, while they are $88 \pm 22\%$, $47 \pm 26\%$, and $32 \pm 27\%$ at -8 , -12 , and -18°C respectively for the supermicron mode. These observations highlight that submicron aerosol particles can contribute to INP concentrations and that the contribution of biological aerosol particles is not negligible, especially when considering the higher number concentrations of submicron particles.

4. Correlations With Atmospheric Parameters

In the following section, we compare the long term WINS data set with collocated atmospheric measurements to determine which aerosol properties can be used to explain INP variability. Correlations between the concentrations of total INPs (INP_{tot}), heat-labile INPs (INP_{HL}), HS INPs (INP_{HS}) with various aerosol physical ($N_{aer,tot}$, $N_{aer,500}$, and S_{aer}) and chemical (Black Carbon BC, inorganic ion concentrations Cl^- , NO_3^- , SO_4^{2-} , Oxalate, Na^+ , NH_4^+ , K^+ , Mg^{2+} , Ca^{2+}) properties were investigated for WINS data (Tables 1 and 2).

The correlations were computed at three temperatures (-12 and -15°C), to better understand the dominant relationships in each of the temperature regimes and to better distinguish between the influencing factors of “cold” and “warm” INPs. HS and HL INPs at -8°C are not included in the following tables, as HS INPs at this temperature represent less than 10% of the total INPs.

4.1. Grouped INP Data

For physical parameters $N_{aer,tot}$ and S_{aer} good relationships ($R^2 > 0.7$) were measured with INP_{tot} at -8°C (Table 1). However, relatively lower correlations are observed for $N_{aer,500}$ ($R^2 \approx 0.35$) with INPs at -8°C . At -12 and -15°C , only HS INPs have significant correlations to $N_{aer,tot}$. It is presumed that concentrations at -8°C are too low to reliably derive correlations with other parameters.

Table 2
Linear Regression Correlations Coefficients (R^2) and p -Values (Pearson's Test) Between Submicron Ice-Nucleating Particles (INP) Concentrations at -8 , -12 , and -15°C (INP_{-8} , INP_{-12} , INP_{-15}) and Aerosol Parameters

	$N_{aer,tot}$	$N_{aer,500}$	S_{aer}	BC	Cl^-	NO_3^-	SO_4^{2-}
$INP_{tot,-8}$	0.30 (0.03)	0.57 (<0.005)	–	–	–	–	0.48 (<0.005)
$INP_{tot,-12}$	0.38 (0.01)	–	–	–	–	–	0.27 (0.02)
$INP_{HS,-12}$	–	–	–	–	–	–	0.59 (<0.005)
$INP_{HL,-12}$	–	–	–	–	–	–	–
$INP_{tot,-15}$	0.30 (0.03)	–	–	–	–	–	0.22 (0.04)
$INP_{HS,-15}$	–	–	–	–	–	–	0.46 (<0.005)
$INP_{HL,-15}$	–	–	–	–	–	–	–
	Ox.	Na^+	NH_4^+	K^+	Mg^{2+}	Ca^{2+}	
$INP_{tot,-8}$	0.76 (<0.005)	–	0.47 (<0.005)	0.38 (<0.005)	0.28 (0.02)	0.21 (0.05)	
$INP_{tot,-12}$	–	0.28 (0.02)	0.28 (0.02)	–	0.29 (0.02)	0.31 (0.01)	
$INP_{HS,-12}$	0.30 (0.02)	0.22 (0.04)	0.63 (<0.005)	0.45 (<0.005)	0.40 (<0.005)	0.40 (<0.005)	
$INP_{HL,-12}$	–	–	–	–	–	–	
$INP_{tot,-15}$	–	–	0.24 (0.03)	–	–	0.23 (0.04)	
$INP_{HS,-15}$	–	0.28 (0.02)	0.48 (<0.005)	0.49 (<0.005)	0.24 (0.03)	0.34 (0.01)	
$INP_{HL,-15}$	–	–	–	–	–	–	

Note. Only significant ($P < 0.05$) correlations are indicated. Values with no significant correlations are indicated as n-dashes. Values with $P < 0.005$ are indicated in bold.

Overall, INP concentrations at the warmest temperatures ($> -12^\circ\text{C}$), have best correlations with the concentrations of species SO_4^{2-} , Oxalate and NH_4^+ ($R^2 > 0.6$), and lower correlations ($R^2 \approx 0.25$) with Na^+ and K^+ , tracers of marine origin and NO_3^- , a compound that may be the result of the reaction of HNO_3 with NaCl. At intermediate temperatures, INP_{-12} correlates ($R^2 \approx 0.2$) with Na^+ and NH_4^+ . For $INP_{HS,-12}$, the correlations with Na^+ and Ca^{2+} (respectively marine and dust tracers), are similar as those with the anthropogenic tracers, while INP_{HL} do not show any significant correlation with the classical chemical tracers measured here. At lower temperatures, INP_{tot} does not correlate with any of the chemical compounds, however, INP_{HS} show low correlations with SO_4^{2-} , Na^+ , NH_4^+ and Ca^{2+} ($R^2 \approx 0.3$).

Given these observations, INP_{tot} and INP_{HL} (at temperatures $> -12^\circ\text{C}$) in our study can be linked with terrestrial and background airmasses (SO_4^{2-} , Oxalate, NH_4^+). Those tracers are also linked, albeit less strongly, with HS INPs. However, INP_{HS} are additionally linked to dust tracers (Ca^{2+}). These results indicate a strong influence from local terrestrial sources. Furthermore, both INP_{HL} (at all temperatures) and INP_{HS} (at colder temperature) are weakly correlated to marine tracers (NaCl). This indicates a possible influence from distant marine sources. INPs of marine origin are suspected to play an important role in cloud formation in the remote ocean environment (DeMott et al., 2016; McCluskey et al., 2018; Wilson et al., 2015), but have never been shown to be important in continental areas where terrestrial sources are considered a major contribution (Burrows et al., 2013; Huang et al., 2021). Atlantic air masses represent about 40%–50% of the air masses during the autumn and winter at PUY (Farah et al., 2018, 2021).

In the following section we examine whether these relationships are driven by submicron and supermicron aerosols.

4.2. Size Segregation

Correlations between the aerosol data (aerosol concentrations and surface) and the submicronic INP data set (INP_{sub}) and the supermicronic INP data set (INP_{sup}) are shown in Tables 2, respectively. The aim of this section is to compare the correlations observed for the full INP data set in the previous section (INP_{all}) and the size-segregated data sets in order to provide more insights on the sources of INPs at PUY.

For INP_{sup} (Table S1 in Supporting Information S1) no correlation is observed with $N_{aer,tot}$ or $N_{aer,500}$. This is surprising in the case of $N_{aer,500}$ as it represents the large aerosols. However, this poor correlation could be explained that the $N_{aer,500}$ is only calculated based on the SMPS channel between 500 and 600 nm and therefore does not represent a real $N_{aer,500}$. Furthermore, despite contributing higher number concentrations, supermicronic INP (Table S1 in Supporting Information S1), only show low correlations between the HS fraction at -15°C and NO_3^- , Na^+ and Mg^{2+} .

At -8°C , INP_{sub} (Table 2) show a weaker correlation ($R^2 = 0.30$) with $N_{aer,tot}$ than INP_{all} ($R^2 = 0.70$), but they show a better correlation with $N_{aer,500}$ ($R^2 = 0.57$ instead of 0.39). This would indicate that most submicron warm INP are measured when the high fractions of submicron aerosols larger than 500 nm are present in the sampled air mass.

Table 2 shows that INP_{sub} correlate across the whole temperature spectrum with a different range of chemical parameters than INP_{all} . Among the marine tracers of supermicronic origin (Cl^- , NO_3^- and Na^+) only Na^+ correlate with total and HS INPs at -12 and -15°C ($R^2 < 0.3$). Tracers of anthropogenic and regional airmasses (NO_3^- , SO_4^{2-}) correlate with all INP classes and temperatures, except for INP_{HL} at -12 and -15°C . Tracers of dust-based aerosols (K^+ , Mg^{2+} , and Ca^{2+}) show correlations in the range of 0.2–0.4 all over the data set, with higher values for INP_{HS} , which is consistent with dust-based INPs being non-biological.

These results show that INPs at PUY have diverse origins, with influences from various anthropogenic, terrestrial, marine, and dust sources. With the available measurements in this study, we observe that the main correlations are driven by aerosol number concentrations. The best correlations were found with anthropogenic and terrestrial tracers, especially at temperatures $> -12^{\circ}\text{C}$. Marine tracers exhibit weak correlations ($R^2 = 0.2$ – 0.3) with a large part of the INP data set, hinting at an influence from distant marine sources. This is consistent with other observations that have shown that marine INPs were less important than dust INPs over continental areas (Burrows et al., 2013; DeMott et al., 2010; Gong et al., 2020).

More physical, chemical or biological data coupled with intensive INP measurements would be needed in order to have a clear understanding of the influence of the chemical and physical composition of INPs at PUY. In particular, being able to differentiate the potential sources with reduced sampling periods would be of great help.

5. Empirical Parameterization

The data collected from this study shows that INPs at PUY are dominated by biogenic particles at warmest temperatures and that their properties can be influenced by nearby sources or being transported by long range airmasses. This following section aims to develop a parametrization using collocated measurements to accurately predict INP concentrations. Current parametrizations that exist using aerosol parameters are compiled with data at temperatures below -20°C (D10, DeMott et al., 2010 and D15, DeMott et al., 2015). Others are optimized specifically for biological aerosols samples such as that of W15 (Wex et al., 2015) and more recently that of Patade et al. (2021). Other parametrizations exist using only temperature such as that of M92 (Meyers et al., 1992), and more recently that of Schneider et al. (2021). Since our measurement temperature range is above -18°C and our aerosols are an internal mixture of several species and not just biological aerosols, our objective was to develop a parameterization optimized for warmer temperatures and using collocated measurements of aerosol particles.

In the following section, we use the INP measurements presented in this work to optimize the previous parameterizations (D15), for temperatures higher than -20°C . This new parameterizations was evaluated against two independent data sets.

5.1. Development of a New Parameterization

The WINS data set was chosen for deriving the parameters as it contains the highest number of data points available. Over 6 months of measurements, there are a total of 20 filter samples collected and analyzed in the temperature range from -5 to -18°C , resulting in 377 data points (averaging data points over 0.5°C). In order to evaluate this newly derived parameterization, it was tested using data collected during the PICNIC field campaign and those collected at the MSA site (15 filters analyzed resulting in a total of 330 points when averaging over 0.5°C).

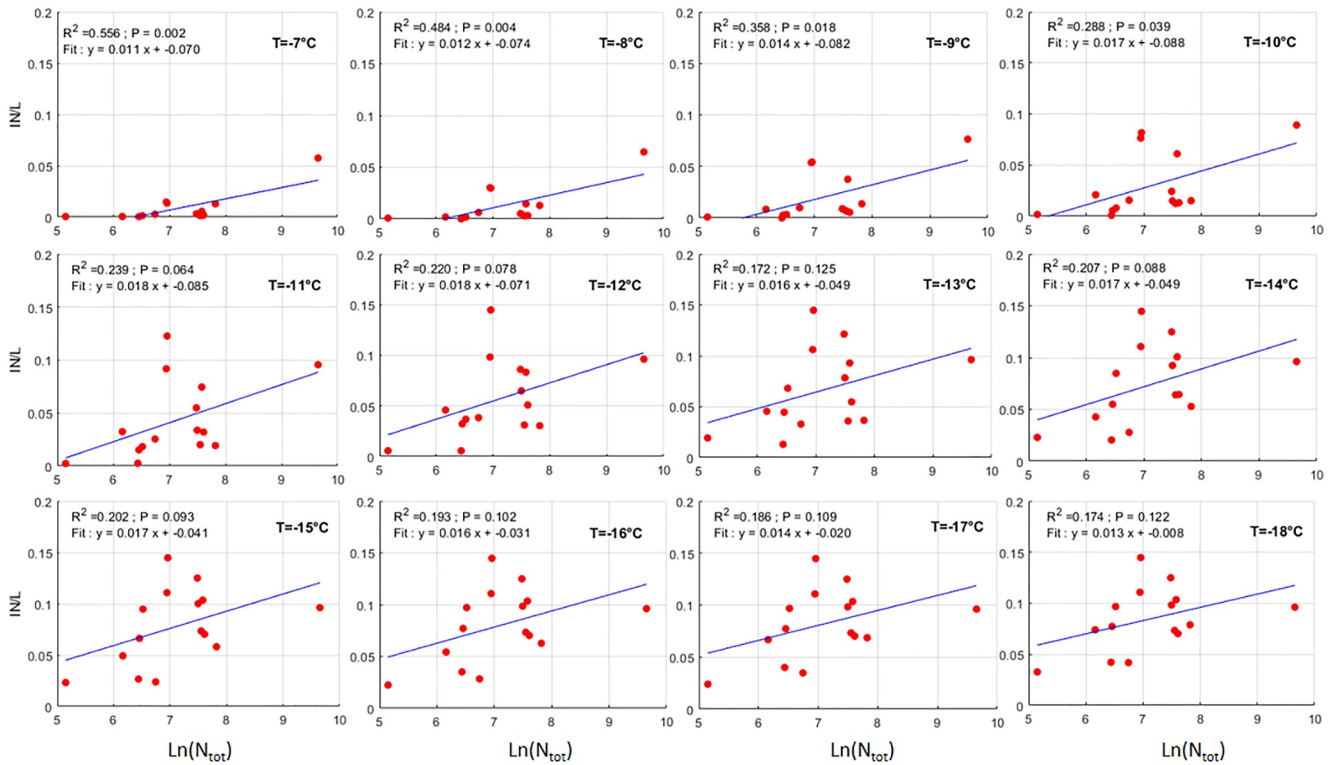


Figure 6. Scatter plots and linear regression fits for ice-nucleating particles (INP) concentrations against $\ln(N_{aer,tot})$. The INP data are averaged over 1°C.

Given the wide use of the D15 parameterization and the ease of optimizing it for our data set, we chose it as the starting point for the development of this new parameterization. Rather than using aerosol number concentration $N_{aer,500}$ as the aerosol variable, we instead used $N_{aer,tot}$. $N_{aer,tot}$ was used as it had good data coverage over the entire sampling period, and had consistently better correlations across all INP spectra compared to with other aerosol variables. Using the total number concentration for the parametrizations is providing us with an easily accessible variable that can be used as a proxy for INP activity. Total number concentration is an aerosol variable required to be measured at a large number of observatory sites within the European ACTRIS network (*Actris.eu*, last access January 2024) but also in other sampling networks (e.g., ASCENT *lascent.research.gatech.edu*, last access: January 2024), GAW (*community.wmo.int/en/activity-areas/gaw/*, last access January 2024), and for the PUY station it is a good indicator of BL air influence (Farah et al., 2018).

In order to adapt the parametrization of D15, we investigated the relationship between $\ln(N_{aer,tot})$ and the INP concentrations at each temperature (Figure 6). Despite the low number of points and the likely influence of some extreme values, we observed the best fit is linear at a given temperature. As observed in Figure 6, these fits become negative under warmest temperatures and low particle concentrations ($<150 \text{ cm}^{-3}$). It is therefore important to note that this fit is not suitable to be used under low number concentrations.

We then replaced $N_{aer,500}$ power law from D15, which also depends on temperature, with a linear function only depending on $\ln(N_{aer,tot})$ (std cm^{-3}) (Equation 3). The final set of parameters was calculated using a Markov chain Monte Carlo algorithm, resulting in the following equation for the new parameterization is:

$$n_{\text{INP}}(T, N_{aer,tot}) = (a * \ln(N_{aer,tot}) + b) * \exp(c * (-T_C) + d), \quad (3)$$

where $a = 0.0489$; $b = -0.2349$; $c = 0.4293$; $d = -6.6477$; T_C the cloud temperature in Celsius and n_{INP} the number of INP per liter of air.

In Figure 7, we plot the predicted data against the observed data, for our parameterizations (referred to as B24). Up to 57.3% of points predicted by our model falls within a factor of 2 of the observed data (RG2). A total of 87.7% of points were predicted within a factor of 5 (RG5) and 98.0% of points were predicted within a factor of 10

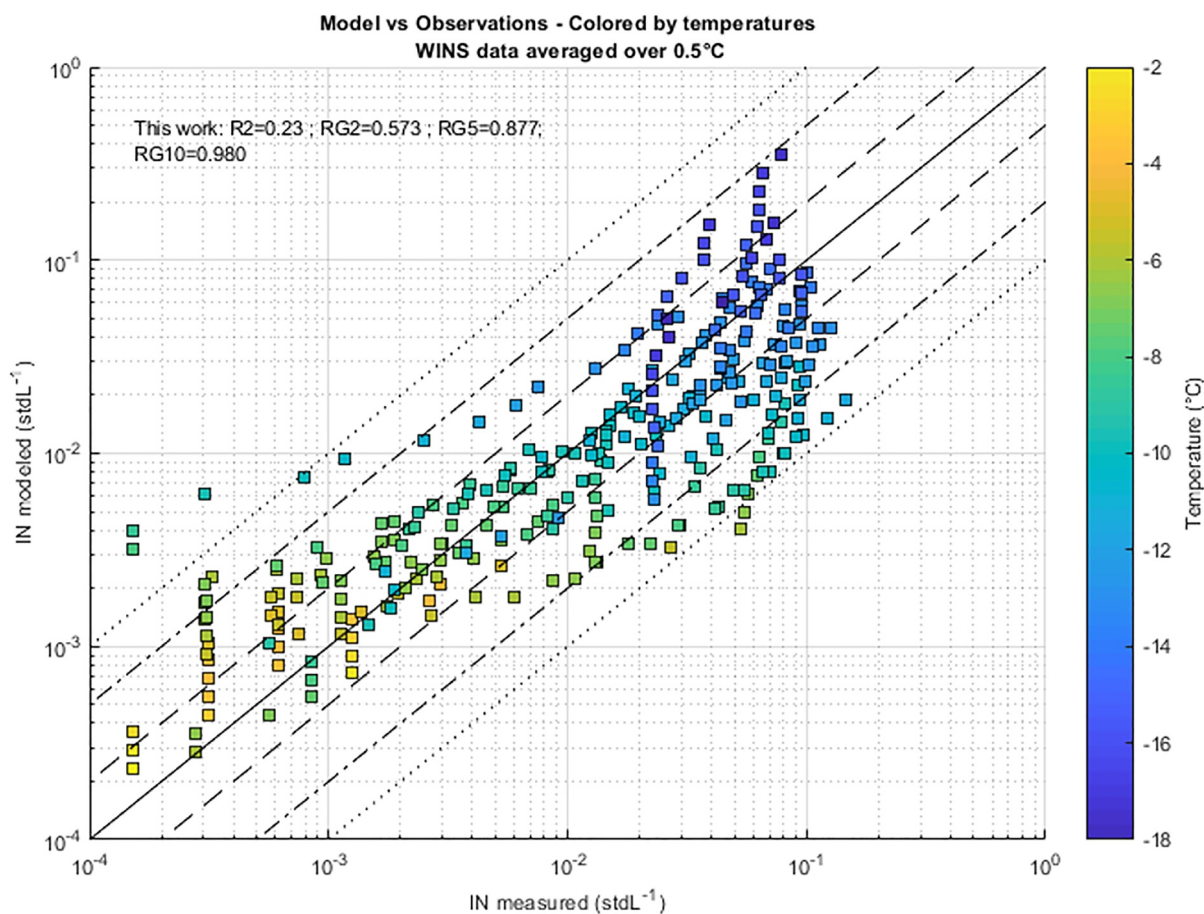


Figure 7. New parameterization from this work (B24) using the data from Weekly Ice Nuclei Samples. The solid line, dashed lines, dash-dotted lines and dotted lines represent respectively the 1:1 ratio line, the 1:2 ratio lines, the 1:5 ratio lines and the 1:10 ratio lines.

(RG10). Highest discrepancies were observed for highest INP concentrations, with an average underestimated by the parameterization for high to intermediate temperatures (-6 to -12°C) and overestimated for low temperatures (below -15°C), illustrating that in some circumstances, factors other than the aerosol number concentration can play an important role for predicting INP concentrations, such as the nature of the particles acting as INP, as shown by the link between aerosol chemistry and INP concentrations discussed Section 4. It is important to consider that a large variability is associated with measurements made at temperatures above -12°C .

5.2. Application on Other Sites

Two independent data sets were combined and used together to test the B24 parameterizations: the data from the PICNIC campaign at the PUY station, and the data from the MSA site from the Pan-European IN sampling campaign. MSA is a continental background site, similar to PUY in terms of altitude, and the availability of the aerosol data during the sampling period allowed us to test the B24 parameterization. MSA INP freezing spectra are similar to that of the PUY measurements, with similar freezing onsets between -4 and -6°C , and concentrations ranging between 10^{-4} and 10^{-1} INP/stdL (Figure S7 in Supporting Information S1). Results show the good ability of the B24 parameterizations to predict INP concentrations, with 38.7% of the INP concentrations predicted within a factor 2%, 86.4% within a factor 5% and 92.8% within a factor 10 (Figure 8).

Predicted data for PICNIC are underestimated at high measured INP concentrations (10^{-2} to 10^{-1} INP/stdL), while for MSA they are overestimated at low concentrations (about 10^{-3} INP/stdL). Both sites exhibit roughly the same INP concentrations (10^{-3} to 10^{-1} INP/stdL), freezing temperatures (-5 to -15°C) and aerosol concentrations (300 – $3,000\text{ cm}^{-3}$).

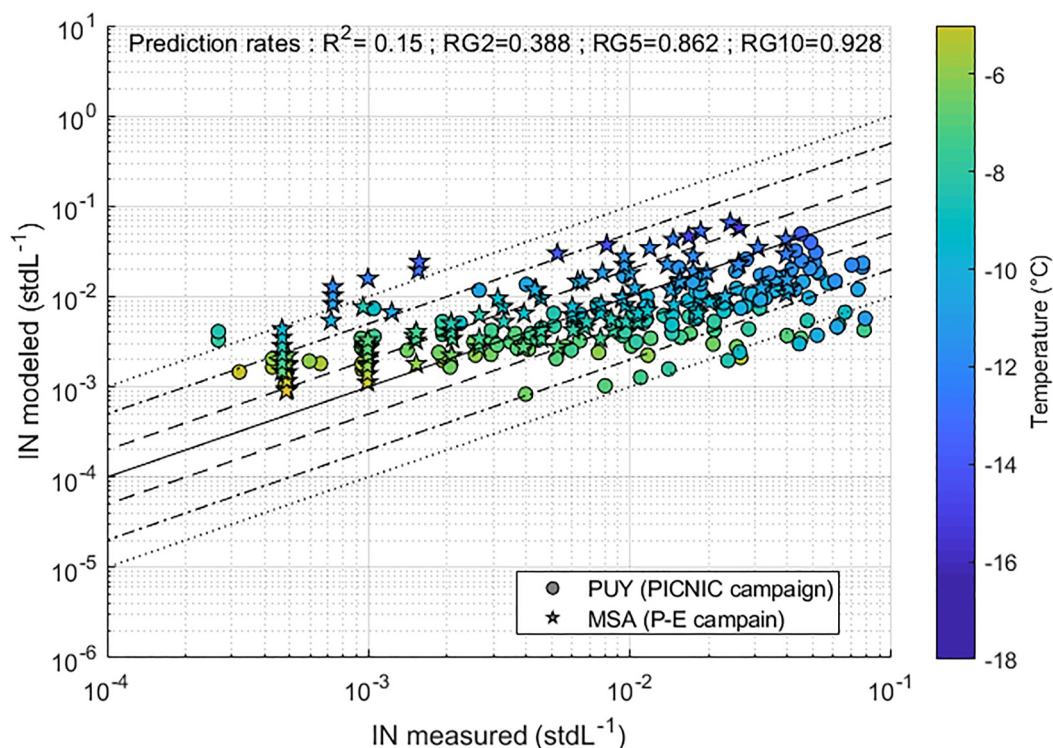


Figure 8. Verification of the new parameterization using the Puy de Dôme Ice Nucleation Intercomparison Campaign and Montsec d’Ares data sets.

6. Conclusions

Diurnal INP measurements were taken during the PICNIC measurement campaign at the observation station at Puy de Dôme in Central France during October 2018. This was followed by the collection of weekly size-segregated INP samples from November 2018 to May 2019 (WINS). These filter samples were extracted into 0.9% NaCl water and were then analyzed using the immersion freezing apparatus LINDA to determine the concentration of INP as a function of temperature. For each filter sample extracted, a fraction of the solution underwent heat treatment to obtain information on the contribution of biological material to INP concentration.

We report INP concentrations between -5 and -18°C and a freezing onset of -4 to -6°C , which are relatively high temperatures in the case of ice nucleation, and have rarely been reported. The observed concentrations are in the range of other measurements from the literature at similar sites and temperatures (Kanji et al., 2017; Mason et al., 2016). Above -10°C , we observe that more than 80% of the INPs are heat labile, and thus potentially of biological origin. At colder temperatures, the ratio of heat labile INPs to total INPs show a contribution of biological INPs representing 40% at -14°C and approximately 10% at -16 to -18°C of the total INP concentration. Two other studies on INPs of biological origin in cloud water and precipitation that took place at PUY have reported ratios of about 100% of biological INPs at -8°C (Joly et al., 2014), to 77% at -12°C (Pouzet et al., 2017), which is much higher than in the aerosol phase in our study. Similar biological fractions are also reported at other mountain sites in snow (T. C. J. Hill et al., 2014) or rain water (Lu et al., 2016), and in other studies in rural (Garcia et al., 2012) or forest sites (Schneider et al., 2021).

Size-segregated data (submicronic and supermicronic INPs) were also analyzed, and in agreement with previous studies we show that supermicronic INPs constituted two thirds of the total INP number. Heat labile INPs were less abundant in the supermicron mode than in the submicron mode. Similar to the seasonal variations in aerosol concentrations, INP concentrations (both heat labile and HS, and sub and supermicronic) had lowest concentrations in winter and highest in autumn and spring. The seasonal variation of aerosol concentrations were reported to be significantly influenced by the seasonal variation of the boundary layer height, reaching the site more

often during the warmer seasons than during winter. The INP concentrations seem to also follow this trend. In addition, snow cover and a decrease in vegetation coverage near the site likely contributed to the higher ratio of HS INPs to total INPs observed in winter.

In order to characterize the impact of aerosol physical and chemical properties on INP concentrations in our study, and to determine the best parameters for deriving a parameterization for INP predictions at temperatures warmer than -20°C , correlations were calculated between INP data (all INPs, heat labile INP, and HS INPs) at three temperatures, (representative of the different regimes (biological, mixed and non-biological) of our data set), and different physical (aerosol numbers and surface concentration) and chemical parameters. In general, significant correlations were measured for INPs at temperatures $>-15^{\circ}\text{C}$. Most notably, we observed that INPs across all temperatures showed consistently significant correlations with $N_{aer,tot}$. We highlight strong links with anthropogenic and terrestrial tracers (SO_4^{2-} , NH_4^+ , Oxalate). Weak correlations were observed with tracers of marine aerosols (Cl^- , Na^+ , NO_3^-).

Correlations with the size-segregated data were also computed. Supermicronic INP did not show significant correlations with any of the studied parameters, while submicronic INPs showed similar significant correlations with the physical variables than the whole data set. Showing that these relationships are driven by aerosol number concentration. Intermediate correlations were also found with marine, dust and anthropogenic tracers for submicronic INPs, which further hints at various possible sources of INPs at PUY.

On the basis of the relationship between INP and the variable $N_{aer,tot}$, the WINS data set was used to develop a new parameterization. The total number concentration of aerosols is a widely available parameter in most studies and observation stations, making it easy to use it as a parameter to predict INP concentrations. This parameterization is optimized for warmer temperatures above -20°C , which are in general dominated by biological activity. This parameterization has been successfully tested on two other similar data sets, one from the PICNIC campaign, and one from Montsec d'Ares (MSA) during the Pan-European INP measurement campaign in 2018.

This study provides INP data and analysis from a remote altitude site which is influenced by long range air masses, and shows that biological INP are of primary importance in such sites. To understand the interactions between aerosols and clouds, it is critical to correctly assess and predict the concentrations of INPs around the globe. Future research activities should focus on performing both long term and size-segregated INP measurements. This information would provide a better link to the INP seasonal variability to local atmospheric properties, and to better characterize dominant sources of INP activity. Additionally, parallel measurements of biological aerosols would assist in better characterizing the link between aerosol biological content and its INP activity. In particular, being able to better differentiate the potential sources of INPs, and thus sampling INPs with higher time resolutions will provide additional information to our understanding of these interactions.

Appendix A: Overview of Past Works on Parameterizing INP Concentrations in the Atmosphere

Studies focusing on the impact of INPs on climate and precipitation relied either on very simplified parameterizations, or by theorizing relations between particle type and IN properties (DeMott et al., 2010). Kanji et al. (2017), provide an in depth description of the different types of parameterizations that have been developed in the past.

Specifically, parameterizations are divided in two types: a time-dependent approach (stochastic effects), such as the time-dependent freezing rate model (Vali & Snider, 2015); and a time-independent approach, which supposes that ice nucleation activity depends only on temperature or aerosol properties such as number concentration (deterministic effects). It has been suggested that the time dependence effects are less important than temperature or aerosol properties dependence (Langham & Mason, 1958; Vali, 2014). The parameterizations we will consider here are of time-independent nature, such as Meyers et al. (1992), which depends only on temperature, or DeMott et al. (2010) and DeMott et al. (2015) which depend on temperature and particle concentrations.

Meyers et al. (1992) (henceforth M92) proposed a simple parameterization of the form:

$$n_{\text{INP}} = \exp(a + b[273.15 - T_C]), \quad (\text{A1})$$

where n_{INP} is the predicted number of INPs and T_C the temperature of the cloud droplet in K.

Based on a global observational data set from CFDC measurements, DeMott et al. (2010) showed that, at temperatures colder than -20°C and for dust INPs, the number of INP was also a function of a power law of the number of aerosols with diameters greater than 500 nm ($N_{\text{aer},500}$). They proposed a parameterization (D10) of the form:

$$n_{\text{INP}} = a(273.15 - T_K)^b \cdot N_{\text{aer},500}^{c(273.15 - T_K) + d}, \quad (\text{A2})$$

with $a = 0.0000594$, $b = 3.33$, $c = 0.0264$, $d = 0.0033$, and T_K the cloud temperature in K.

Tobo et al. (2013) also proposed a parameterization based on $N_{\text{aer},500}$, but taking into account the number of fluorescent biological aerosol particles. This parameterization has been further modified in DeMott et al. (2015) (D15) as:

$$n_{\text{INP}} = (\text{cf}) N_{\text{aer},500}^{\alpha(273.15 - T_K) + \beta} \cdot \exp(\gamma[273.15 - T_K] + \delta), \quad (\text{A3})$$

with $\text{cf} = 1$, $\alpha = 0$, $\beta = 1.25$, $\gamma = 0.46$, $\delta = -11.6$.

Niemand et al. (2012) developed a parameterization (N12) for immersion freezing of desert dust particles based on the surface site density of INP (n_S , in INP/m^2) formulated as:

$$n_S = \exp(0.517[T_K - 273.15] + 8.934). \quad (\text{A4})$$

Wex et al. (2015) developed a parameterization (W15) aimed for predicting biological INPs, using Snomax[®] as a reference, and calculating surface site density n_S . Snomax[®] is an artificially-made aerosol based on the proteins of natural bacteria that act as ice nucleation initiators. The n_S predicted by W15 is as follows:

$$n_S = \frac{(1.4 \times 10^{12}) [1 - \exp(-2.00 \times 10^{-10}) \exp(-2.34 \times T)]}{\text{geometric SSA}_{\text{Snowmax}}}, \quad (\text{A5})$$

with a value of $7.99 \text{ m}^2 \text{ g}^{-1}$ for geometric SSA of Snomax[®], which is taken from AIDA measurements in Hir-anuma et al. (2019).

One drawback of the D15 and the D10 is that they are optimized from measurements with a continuous flow diffusion chamber with operating temperatures lower than -20°C . Therefore, they are weakly constrained for temperatures warmer than -20°C . Furthermore, because they consider only larger aerosols at lower temperatures, the D10 and D15 parameterizations implicitly tend to consider only mineral dust. As a result of the simplicity of this parameterizations, and of the widespread availability of aerosol number concentrations, a number of studies have optimized this parameterizations for their data, corresponding to specific environments. For example, Schneider et al. (2021) worked from D15 in order to derive parameterizations coefficients predicting INPs in a boreal forest, an environment rich in biological aerosols. They reported an agreement of about 90%–99% (80%–95% and 41%–57%) within a factor of 10 (5 and 2) was reported between the observations and predictions, depending on the season.

Data Availability Statement

The INP data used in the study is available in the AERIS database under the “Puy de Dôme” file: <https://doi.org/10.25326/664>. The 2018–2019 aerosol parameters data measured at PUY (aerosol number concentrations, aerosol surfaces, inorganics concentrations, carbon concentrations) are stored in the EBAS database under the following link: <http://ebas.data.nilu.no>.

Acknowledgments

This research received funding from the European Commission under the Horizon 2020-Research and Innovation Framework Program via the ACTRIS-2 Trans-National Access, and from the ANR-CHAIN (ANR 14-CE01-0003-01). The authors gratefully acknowledge CNRS-INSU for supporting measurements performed at the SI-COPDD, and those within the long-term monitoring aerosol program SNO-CLAP, both of which are components of the ACTRIS French Research Infrastructure, and whose data is hosted at the AERIS data center (<https://www.aeris-data.fr>). We thank E.B. for the discussions for deriving the parameterization.

References

- Atkinson, J. D., Murray, B. J., Woodhouse, M. T., Whale, T. F., Baustian, K. J., Carslaw, K. S., et al. (2013). The importance of feldspar for ice nucleation by mineral dust in mixed-phase clouds. *Nature*, *498*(7454), 355–358. <https://doi.org/10.1038/nature12278>
- Baray, J.-L., Deguillaume, L., Colomb, A., Sellegri, K., Freney, E., Rose, C., et al. (2020). C ezeaux-Aulnat-Opme-Puy De D ome: A multi-site for the long-term survey of the tropospheric composition and climate change. *Atmospheric Measurement Techniques*, *13*(6), 3413–3445. <https://doi.org/10.5194/amt-13-3413-2020>
- Beall, C. M., Lucero, D., Hill, T. C., DeMott, P. J., Stokes, M. D., & Prather, K. A. (2020). Best practices for precipitation sample storage for offline studies of ice nucleation in marine and coastal environments. *Atmospheric Measurement Techniques*, *13*(12), 6473–6486. <https://doi.org/10.5194/amt-13-6473-2020>
- Boucher, O., & Randall, D. (2013). Clouds and aerosols. In *Climate change 2013: The physical science basis. Contribution of working group I to the fifth assessment report of the intergovernmental panel on climate change*.
- Bourcier, L., Sellegri, K., Chausse, P., Pichon, J. M., & Laj, P. (2012). Seasonal variation of water-soluble inorganic components in aerosol size-segregated at the puy de D ome station (1,465 m a.s.l.), France. *Journal of Atmospheric Chemistry*, *69*(1), 47–66. <https://doi.org/10.1007/s10874-012-9229-2>
- Burrows, S. M., Easter, R. C., Liu, X., Ma, P.-L., Wang, H., Elliott, S. M., et al. (2022). OCEANFILMS (Organic Compounds from Ecosystems to Aerosols): Natural Films and Interfaces via Langmuir Molecular Surfactants) sea spray organic aerosol emissions – implementation in a global climate model and impacts on cloudss. *Atmospheric Chemistry and Physics*, *22*, 5223–5251. <https://doi.org/10.5194/acp-22-5223-2022>
- Burrows, S. M., Hoose, C., P oschl, U., & Lawrence, M. G. (2013). Ice nuclei in marine air: Biogenic particles or dust? *Atmospheric Chemistry and Physics*, *13*(1), 245–267. <https://doi.org/10.5194/acp-13-245-2013>
- Christner, B. C., Cai, R., Morris, C. E., McCarter, K. S., Foreman, C. M., Skidmore, M. L., et al. (2008). Geographic, seasonal, and precipitation chemistry influence on the abundance and activity of biological ice nucleators in rain and snow. *Proceedings of the National Academy of Sciences*, *105*(48), 18854–18859. <https://doi.org/10.1073/pnas.0809816105>
- Conen, F., Einbock, A., Mignani, C., & H uglin, C. (2022). Measurement report: Ice-nucleating particles active $\geq -15^\circ\text{C}$ in free tropospheric air over western Europe. *Atmospheric Chemistry and Physics*, *22*(5), 3433–3444. <https://doi.org/10.5194/acp-22-3433-2022>
- Creamean, J. M., Kirpes, R. M., Pratt, K. A., Spada, N. J., Maahn, M., de, G., et al. (2018). Marine and terrestrial influences on ice nucleating particles during continuous springtime measurements in an Arctic oil field location. *Atmospheric Chemistry and Physics*, *20*, 18023–18042. <https://doi.org/10.5194/acp-18-18023-2018>
- DeMott, P. J., Hill, T. C. J., McCluskey, C. S., Prather, K. A., Collins, D. B., Sullivan, R. C., et al. (2016). Sea spray aerosol as a unique source of ice nucleating particles. *Proceedings of the National Academy of Sciences*, *113*(21), 5797–5803. <https://doi.org/10.1073/pnas.1514034112>
- DeMott, P. J., M ohler, O., Cziczto, D. J., Hiranuma, N., Petters, M. D., Petters, S. S., et al. (2018). The fifth international workshop on ice nucleation phase 2 (FIN-02): Laboratory intercomparison of ice nucleation measurements. *Atmospheric Measurement Techniques*, *11*, 6231–6257. <https://doi.org/10.5194/amt-11-6231-2018>
- DeMott, P. J., M ohler, O., Stetzer, O., Vali, G., Levin, Z., Petters, M. D., et al. (2011). Resurgence in ice nuclei measurement research. *Bulletin of the American Meteorological Society*, *92*(12), 1623–1635. <https://doi.org/10.1175/2011BAMS3119.1>
- DeMott, P. J., Prenni, A. J., Liu, X., Kreidenweis, S. M., Petters, M. D., Twohy, C. H., et al. (2010). Predicting global atmospheric ice nuclei distributions and their impacts on climate. *Proceedings of the National Academy of Sciences*, *107*(25), 11217–11222. <https://doi.org/10.1073/pnas.0910818107>
- DeMott, P. J., Prenni, A. J., McMeeking, G. R., Sullivan, R. C., Petters, M. D., Tobo, Y., et al. (2015). Integrating laboratory and field data to quantify the immersion freezing ice nucleation activity of mineral dust particles. *Atmospheric Chemistry and Physics*, *15*(1), 393–409. <https://doi.org/10.5194/acp-15-393-2015>
- Ealo, M., Alastuey, A., Ripoll, A., P erez, N., Minguill on, M. C., Querol, X., & Pandolfi, M. (2016). Detection of Saharan dust and biomass burning events using near-real-timeintensive aerosol optical properties in the north-western Mediterranean. *Atmospheric Chemistry and Physics*, *16*(19), 12567–12586. <https://doi.org/10.5194/acp-16-12567-2016>
- Farah, A., Freney, E., Canonaco, F., Pr ev ot, A. S. H., Pichon, J., Abboud, M., et al. (2021). Altitude aerosol measurements in Central France: Seasonality, sources and free-troposphere/boundary layer segregation. *Earth and Space Science*, *8*(3), e2019EA001018. <https://doi.org/10.1029/2019EA001018>
- Farah, A., Freney, E., Chauvign e, A., Baray, J.-L., Rose, C., Picard, D., et al. (2018). Seasonal variation of aerosol size distribution data at the Puy de D ome station with emphasis on the boundary layer/free troposphere segregation. *Atmosphere*, *9*(7), 244. <https://doi.org/10.3390/atmos9070244>
- Fletcher, N. H. (1962). Surface structure of water and ice. *Philosophical Magazine*, *7*(74), 255–269. <https://doi.org/10.1080/14786436208211860>
- Freney, E., Sellegri Karine, S. K., Eija, A., Clemence, R., Aurelien, C., Jean-Luc, B., et al. (2016). Experimental evidence of the feeding of the free troposphere with aerosol particles from the mixing layer. *Aerosol and Air Quality Research*, *16*(3), 702–716. <https://doi.org/10.4209/aaqr.2015.03.0164>
- Gabey, A., Vaitilingom, M., Freney, E., Boulon, J., Sellegri, K., Gallagher, M., et al. (2013). Observations of fluorescent and biological aerosol at a high-altitude site in central France. *Atmospheric Chemistry and Physics*, *13*(15), 7415–7428. <https://doi.org/10.5194/acp-13-7415-2013>
- Garcia, E., Hill, T. C. J., Prenni, A. J., DeMott, P. J., Franc, G. D., & Kreidenweis, S. M. (2012). Biogenic ice nuclei in boundary layer air over two U.S. High plains agricultural regions: Biogenic ice nuclei over two agricultural regions. *Journal of Geophysical Research*, *117*(D18), 106. <https://doi.org/10.1029/2012JD018343>
- Gong, X., Wex, H., van Pinxteren, M., Triesch, N., Fomba, K. W., Lubitz, J., et al. (2020). Characterization of aerosol particles at Cabo Verde close to sea level and at the cloud level—Part 2: Ice-nucleating particles in air, cloud and seawater. *Atmospheric Chemistry and Physics*, *20*(3), 1451–1468. <https://doi.org/10.5194/acp-20-1451-2020>
- Gute, E., Lacher, L., Kanji, Z. A., Kohl, R., Curtius, J., Weber, D., et al. (2019). Field evaluation of a Portable Fine Particle Concentrator (PFPC) for ice nucleating particle measurements. *Aerosol Science and Technology*, *53*(9), 1067–1078. <https://doi.org/10.1080/02786826.2019.1626346>
- Hartmann, D., Ockert-Bell, M., & Michelsen, M. (1992). The effect of cloud type on earth’s energy balance: Global analysis. *Journal of Climate*, *5*(11), 1281–1304. [https://doi.org/10.1175/1520-0442\(1992\)005<1281:teocto>2.0.co;2](https://doi.org/10.1175/1520-0442(1992)005<1281:teocto>2.0.co;2)
- Hartmann, M., Blunier, T., Br ugger, S., Schmale, J., Schwikowski, M., Vogel, A., et al. (2019). Variation of ice nucleating particles in the European arctic over the last centuries. *Geophysical Research Letters*, *46*(7), 4007–4016. <https://doi.org/10.1029/2019GL082311>
- Hill, T. C. J., DeMott, P. J., Tobo, Y., Fr ohlich-Nowoisky, J., Moffett, B. F., Franc, G. D., & Kreidenweis, S. M. (2016). Sources of organic ice nucleating particles in soils. *Atmospheric Chemistry and Physics*, *16*(11), 7195–7211. <https://doi.org/10.5194/acp-16-7195-2016>

- Hill, T. C. J., Moffett, B. F., DeMott, P. J., Georgakopoulos, D. G., Stump, W. L., & Franc, G. D. (2014). Measurement of ice nucleation-active bacteria on plants and in precipitation by quantitative PCR. *Applied and Environmental Microbiology*, *80*(4), 1256–1267. <https://doi.org/10.1128/AEM.02967-13>
- Hiranuma, N., Adachi, K., Bell, D. M., Belosi, F., Beydoun, H., Bhaduri, B., et al. (2019). A comprehensive characterization of ice nucleation by three different types of cellulose particles immersed in water. *Atmospheric Chemistry and Physics*, *19*(7), 4823–4849. <https://doi.org/10.5194/acp-19-4823-2019>
- Huang, S., Hu, W., Chen, J., Wu, Z., Zhang, D., & Fu, P. (2021). Overview of biological ice nucleating particles in the atmosphere. *Environment International*, *146*, 106197. <https://doi.org/10.1016/j.envint.2020.106197>
- Huffman, J. A., Prenni, A. J., DeMott, P. J., Pöhlker, C., Mason, R. H., Robinson, N. H., et al. (2013). High concentrations of biological aerosol particles and ice nuclei during and after rain. *Atmospheric Chemistry and Physics*, *13*, 6151–6164. <https://doi.org/10.5194/acp-13-6151-2013>
- Joly, M., Amato, P., Deguillaume, L., Monier, M., Hoose, C., & Delort, A.-M. (2014). Quantification of ice nuclei active at near 0°C temperatures in low-altitude clouds at the Puy de Dôme atmospheric station. *Atmospheric Chemistry and Physics*, *14*(15), 8185–8195. <https://doi.org/10.5194/acp-14-8185-2014>
- Kanji, Z. A., Ladino, L. A., Wex, H., Boose, Y., Burkert-Kohn, M., Cziczko, D. J., & Krämer, M. (2017). Overview of ice nucleating particles. *Meteorological Monographs*, *58*, 1.1–1.33. <https://doi.org/10.1175/AMSMONOGRAPHS-D-16-0006.1>
- Lacher, L., Adams, M., Barry, K., Bertozzi, B., Bingemer, H., Boffo, C., et al. (2024). The puy de dôme ice nucleation intercomparison campaign (picnic): Comparison between online and offline methods in ambient air. *Atmospheric Chemistry and Physics*, *24*, 12345. <https://doi.org/10.5194/egusphere-2023-1125>
- Ladino, L. A., Raga, G. B., Alvarez-Ospina, H., Andino-Enríquez, M. A., Rosas, I., Martínez, L., et al. (2019). Ice-nucleating particles in a coastal tropical site. *Atmospheric Chemistry and Physics*, *19*(9), 6147–6165. <https://doi.org/10.5194/acp-19-6147-2019>
- Langham, E., & Mason, B. J.-N. (1958). The heterogeneous and homogeneous nucleation of supercooled water. *Proceedings of the Royal Society of London. Series A. Mathematical and Physical Sciences*, *247*(1251), 493–504.
- Lohmann, U., & Feichter, J. (2005). Global indirect aerosol effects: A review. *Atmospheric Chemistry and Physics*, *24*, 715–737.
- Lu, Z., Du, P., Du, R., Liang, Z., Qin, S., Li, Z., & Wang, Y. (2016). The diversity and role of bacterial ice nuclei in rainwater from mountain sites in China. *Aerosol and Air Quality Research*, *16*, 640–652. <https://doi.org/10.4209/aaqr.2015.05.0315>
- Maki, L. R., Galyan, E. L., Chang-Chien, M.-M., & Caldwell, D. R. (1974). Ice nucleation induced by *Pseudomonas syringae*l. *Applied Microbiology*, *28*, 4. <https://doi.org/10.1128/am.28.3.456-459.1974>
- Mason, R. H., Si, M., Chou, C., Irish, V. E., Dickie, R., Elizondo, P., et al. (2016). Size-resolved measurements of ice-nucleating particles at six locations in North America and one in Europe. *Atmospheric Chemistry and Physics*, *16*(3), 1637–1651. <https://doi.org/10.5194/acp-16-1637-2016>
- McCluskey, C. S., Hill, T. C. J., Malfatti, F., Sultana, C. M., Lee, C., Santander, M. V., et al. (2017). A dynamic link between ice nucleating particles released in nascent sea spray aerosol and oceanic biological activity during two Mesocosm experiments. *Journal of the Atmospheric Sciences*, *74*(1), 151–166. <https://doi.org/10.1175/JAS-D-16-0087.1>
- McCluskey, C. S., Ovadnevaite, J., Rinaldi, M., Atkinson, J., Belosi, F., Ceburnis, D., et al. (2018). Marine and terrestrial organic ice-nucleating particles in Pristine marine to continentally influenced Northeast Atlantic air masses. *Journal of Geophysical Research: Atmospheres*, *123*(11), 6196–6212. <https://doi.org/10.1029/2017JD028033>
- Meyers, M., DeMott, P. J., & Cotton, W. R. (1992). New primary ice-nucleation parametrizations in an explicit cloud model. *American meteorological society*, *31*(7), 708–721. <https://doi.org/10.1175/1520-0450>
- Murray, B. J., O’Sullivan, D., Atkinson, J. D., & Webb, M. E. (2012). Ice nucleation by particles immersed in supercooled cloud droplets. *Chemical Society Reviews*, *41*(19), 6519. <https://doi.org/10.1039/c2cs35200a>
- Niemand, M., Möhler, O., Vogel, B., Vogel, H., Hoose, C., Connolly, P., et al. (2012). A particle-surface-area-based parameterization of immersion freezing on desert dust particles. *Journal of the Atmospheric Sciences*, *69*(10), 3077–3092. <https://doi.org/10.1175/JAS-D-11-0249.1>
- O’Sullivan, D., Adams, M. P., Tarn, M. D., Harrison, A. D., Vergara-Temprado, J., Porter, G. C. E., et al. (2018). Contributions of biogenic material to the atmospheric ice-nucleating particle population in North Western Europe. *Scientific Reports*, *8*(1), 13821. <https://doi.org/10.1038/s41598-018-31981-7>
- Patade, S., Phillips, V. T. J., Amato, P., Bingemer, H. G., Burrows, S. M., DeMott, P. J., et al. (2021). Empirical formulation for multiple groups of primary biological ice nucleating particles from field observations over Amazonia. *Journal of the Atmospheric Sciences*. <https://doi.org/10.1175/JAS-D-20-0096.1>
- Picard, D. (2021). libszdist. (swlh:1:dir:7057a716afab8ca80728aa7c6c2cc4bd03b0f45b;origin=https://hal.archives-ouvertes.fr/hal-01883795;visit=swlh:1:snp:e59379a4f88c297066e964703893c23b08264ec8;anchor=swlh:1:rel:fc8e44c5bb3fabe81e5ebe46ac013a2510271616;path=/). (hal-01883795v2).
- Pouzet, G., Peghaire, E., Aguès, M., Baray, J.-L., Conen, F., & Amato, P. (2017). Atmospheric processing and variability of biological ice nucleating particles in precipitation at Opme, France. *Atmosphere*, *229*(11), 229. <https://doi.org/10.3390/atmos8110229>
- Pruppacher, H. R. (2010). *Microphysics of clouds and precipitation* (2nd.edn.). Springer.
- Ripoll, A., Minguillón, M. C., Pey, J., Jimenez, J. L., Day, D. A., Querol, X., & Alastuey, A. (2014). Long-term real-time chemical characterization of submicron aerosols at Montsec (Southern Pyrenees, 1570 m a.s.l.). *Aerosols/Field Measurements/Troposphere/Chemistry (chemical composition and reactions)*. <https://doi.org/10.5194/acpd-14-28809-2014>
- Ripoll, A., Pey, J., Minguillón, M. C., Pérez, N., Pandolfi, M., Querol, X., & Alastuey, A. (2014). Three years of aerosol mass, black carbon and particle number concentrations at Montsec (southern Pyrenees, 1570 m a.s.l.). *Atmospheric Chemistry and Physics*, *14*(8), 4279–4295. <https://doi.org/10.5194/acp-14-4279-2014>
- Schneider, J., Höhler, K., Heikkilä, P., Keskinen, J., Bertozzi, B., Bogert, P., et al. (2021). The seasonal cycle of ice-nucleating particles linked to the abundance of biogenic aerosol in boreal forests. *Atmospheric Chemistry and Physics*, *21*(5), 3899–3918. <https://doi.org/10.5194/acp-21-3899-2021>
- Schrod, J., Thomson, E. S., Weber, D., Kossmann, J., Pöhlker, C., Saturno, J., et al. (2020). Long-term deposition and condensation ice-nucleating particle measurements from four stations across the globe. *Atmospheric Chemistry and Physics*, *20*(24), 15983–16006. <https://doi.org/10.5194/acp-20-15983-2020>
- Stopelli, E., Conen, F., Zimmermann, L., Alewell, C., & Morris, C. E. (2014). Freezing nucleation apparatus puts new slant on study of biological ice nucleators in precipitation. *Atmospheric Measurement Techniques*, *7*(1), 129–134. <https://doi.org/10.5194/amt-7-129-2014>
- Tobo, Y., Adachi, K., DeMott, P. J., Hill, T. C. J., Hamilton, D. S., Mahowald, N. M., et al. (2019). Glacially sourced dust as a potential significant source of ice 2 nucleating particles. *Nature Geoscience*, *12*(4), 253–258. <https://doi.org/10.1038/s41561-019-0314-x>

- Tobo, Y., Prenni, A. J., DeMott, P. J., Huffman, J. A., McCluskey, C. S., Tian, G., et al. (2013). Biological aerosol particles as a key determinant of ice nuclei populations in a forest ecosystem: Biological ice nuclei in forest. *Journal of Geophysical Research: Atmospheres*, *118*(17), 10100–10110. <https://doi.org/10.1002/jgrd.50801>
- Ullrich, R., Hoose, C., Möhler, O., Niemand, M., Wagner, R., Höhler, K., et al. (2017). A new ice nucleation active site parameterization for desert dust and Soot. *Journal of the Atmospheric Sciences*, *74*(3), 699–717. <https://doi.org/10.1175/JAS-D-16-0074.1>
- Vali, G. (1971). Quantitative evaluation of experimental results on the heterogenous freezing nucleation of supercooled liquids. *Journal of the Atmospheric Sciences*, *28*(3), 402–409. [https://doi.org/10.1175/1520-0469\(1971\)028<0402:qeoera>2.0.co;2](https://doi.org/10.1175/1520-0469(1971)028<0402:qeoera>2.0.co;2)
- Vali, G. (2014). Interpretation of freezing nucleation experiments: Singular and stochastic; sites and surfaces. *Atmospheric Chemistry and Physics*, *14*(11), 5271–5294. <https://doi.org/10.5194/acp-14-5271-2014>
- Vali, G., & Snider, J. R. (2015). Time-dependent freezing rate parcel model. *Atmospheric Chemistry and Physics*, *15*(4), 2071–2079. <https://doi.org/10.5194/acp-15-2071-2015>
- Venzac, H., Sellegri, K., Villani, P., Picard, D., & Laj, P. (2009). Seasonal variation of aerosol size distributions in the free troposphere and residual layer at the puy de Dôme station, France. *Atmospheric Chemistry and Physics*, *9*(4), 1465–1478. <https://doi.org/10.5194/acp-9-1465-2009>
- Wex, H., Augustin-Bauditz, S., Boose, Y., Budke, C., Curtius, J., Diehl, K., et al. (2015). Intercomparing different devices for the investigation of ice nucleating particles using Snomax[®] as test substance. *Atmospheric Chemistry and Physics*, *15*(3), 1463–1485. <https://doi.org/10.5194/acp-15-1463-2015>
- Wilson, T. W., Ladino, L. A., Alpert, P. A., Breckels, M. N., Brooks, I. M., Browse, J., et al. (2015). A marine biogenic source of atmospheric ice-nucleating particles. *Nature*, *525*(7568), 234–238. <https://doi.org/10.1038/nature14986>
- Wolf, M. J., Zhang, Y., Zawadowicz, M. A., Goodell, M., Froyd, K., Freney, E., et al. (2020). A biogenic secondary organic aerosol source of cirrus ice nucleating particles. *Nature Communications*, *11*(1), 4834. <https://doi.org/10.1038/s41467-020-18424-6>